Chapter 5

Modeling Nutrient Upwelling in Lake Malawi/Nyasa

P.F.Hamblin
Environment Canada, National Water Research Institute, P.O. Box 5050, Burlington, ON L7R 4A6, Canada

H.A. Bootsma
SADC/GEF Lake Malawi/Nyasa Biodiversity Conservation Project, P.O. Box 311, Salima, Malawi

R.E.Hecky
Environment Canada, National Water Research Institute, P.O. Box 5050, Burlington, ON L7R 4A6, Canada

Introduction

While there are many factors influencing primary production in lakes, nutrient availability is likely to be the dominant factor (Guildford et al., Chapter 6), especially in lakes where the fish species are intensively harvested such as is the case of Lake Malawi/Nyasa. While some measurements of the lake's nutrient distributions have been made previously (Beauchamp 1953; Jackson et al. 1963; Bootsma 1993; Patterson and Kachinjika 1995), a better understanding of nutrient cycling is required to fully assess the fisheries potential of the lake, to shed light on the principles responsible for sustaining the lake's unique biodiversity of fish species, and to predict the potential impacts of changes in nutrient fluxes to the lake.

The purpose of this study is to expand on the earlier nutrient measurements and to investigate the possible mechanisms of nutrient cycling in Lake Malawi/Nyasa. It is considered that nutrients are renewed in the photic zone by vertical transport from the nutrient-rich deeper waters of the lake. Even though dissolved nutrients are apt to be assimilated rapidly in the photic zone, recycling and retention of nutrients can result in chemical and biological effects that are spatially and temporally dissociated from a vertical mixing event. Thus, it is necessary not only to determine the vertical transport of nutrients but also the horizontal transport of matter in the photic zone. In this chapter we have neglected the roles of incoming rivers and streams and atmospheric deposition in the nutrient budget of the lake as this topic is examined in Chapters 2, 3 and 8.

Vertical transport of nutrients can be accomplished by two mechanisms, namely, by upward flow (or upwelling) and by turbulent transport. The second process may be further classified into down gradient transport due to the weak turbulent mixing in the interior of the water column and into vertical entrainment of higher nutrient concentrations into the near-surface mixed layer. Unfortunately, none of these mechanisms can be directly measured with the exception of the horizontal flow in the mixed layer. In the present study, even this was beyond our resources to observe. Instead, we employed indirect methods of inferring the desired transports by means of a mathematical model, field observations of wind and water temperatures, and some assumptions about the strength of vertical

Acknowledgments – We are grateful for the assistance of Mr. S. Smith, Captain M. Day and the crew of R/V Usipa in deploying and retrieving thermistor moorings. We also thank Mr. R. Tymowski for his help with data analysis.

mixing in the deeper layers of the lake. Unfortunately at this stage of analysis, the results of mixing tracer studies (Chapter 4) cannot provide quantitative estimates of these vertical mixing coefficients.

Methods and Primary Observations

Field Measurements - At up to four stations located on the shoreline of Lake Malawi/Nyasa (see Fig. 5.1) complete sets of surface meteorological observations were taken at 10-min (Chilumba and *Usipa*) or 30-min (Senga Bay and Likoma) intervals starting in early 1997. However, only the wind speed and direction are of concern in the present study. Depending on the operation of temperature recorders, profiles of water temperature at 20-min sampling rates were observed concurrently at as many as four moorings, again over the same period as the meteorological stations. The horizontal placement of the moorings is indicated in Figure 5.1 and the vertical position of the temperature loggers in Figure 5.2. At some moorings, sediment traps collected sinking particulate material. It is hoped that the monitoring of meteorological conditions, lake thermal structure, and sedimentation will continue over the next several years in order to evaluate interannual differences in primary production and their relation to the causative factors.

An AVHRR (advanced very high resolution radiometer) satellite receiver located at the Senga Bay research station collected lake images twice daily when cloud cover permitted. Preliminary calibration with *in situ* measurements indicates that lake surface temperatures derived from these images are accurate to within <0.5 °C. When considered along with the surface temperature recorders, these satellite observations offer detailed distributions of horizontal thermal gradients.

Winds. Figure 5.3 shows a typical behaviour of the individual wind readings over a weekly period at a shoreline location. It is evident that there is much variation in wind speed and direction over a daily period. However, when the winds are plotted as daily vector averages as in Figure 5.4, a more persistent pattern emerges at all stations. Figure 5.5 presents the product of the wind speed and the component of the wind along the longitudinal axis of the lake, with 0° being taken as positive and a constant of proportionality. This quantity corresponds to the tangential force of the wind along the major axis of the lake and is thought to be representative of the southern portion of the lake in the vicinity of the Senga Bay station. The wind force is remarkably persistent and hardly ever becomes negative over the 430 days (14 months) studied to date. The winds tend to be strongest in the period of May through to October and weakest from November to March. The most significant storm events have durations of about 10 days. The peak wind stress occurred in June.

Temperatures. Once the individual pre-field calibrations were applied to the temperature recorders, daily-averaged profiles of temperature were plotted for each mooring over the 14-month study period in order to identify any possible errors. Depths of the sensors were determined from one instrument mounted close to the surface that measured hydrostatic pressure or depth (marked 'D' on Figure 5.2) and the rest of the depths worked out from known cable lengths. A typical plot of staggered temperature profiles is shown in Figure 5.6 and demonstrates the development of the stratification in November and December in the southern portion of the lake. After the instruments are retrieved they will undergo a post-field calibration.

After correcting for errors and eliminating erroneous data, contours of the evolution of the isotherms over the experimental period show some interesting features at the two stations in the southern extremity of the lake (Figures 5.7 and 5.8). In general, temperatures at the more southern of the two stations, mooring number one (THRM1, Fig. 5.1) are colder than at station 2 (THRM2) and have a longer period of nearly isothermal conditions in the austral winter. Both have episodic events where colder water is brought close to the surface, with the event in March 1998 being the most notable. Both stations have some evidence of an approximately 18-day periodicity in vertical isotherm displacements. However, since this period is so close to the duration of the major wind events, identification of the 18-day period with the internal seiche is problematic at this time. Previous studies have suggested internal seiche periods ranging from 16 to 30 days (Jackson et al. 1963; Eccles 1974).

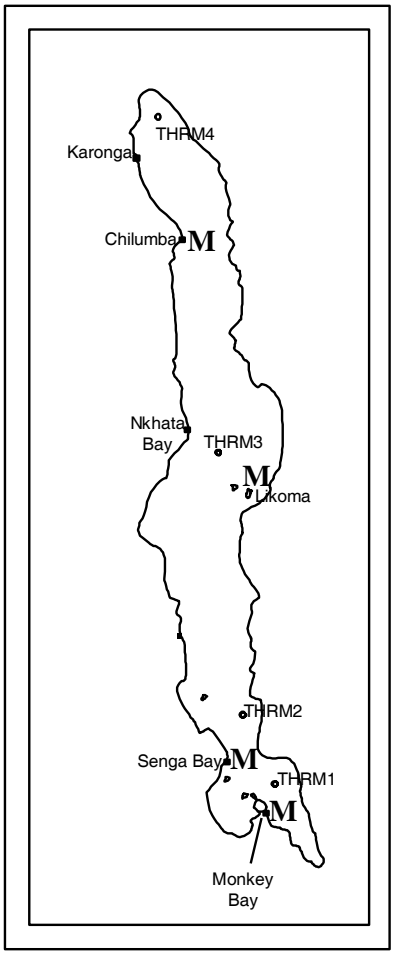

Fig. 5.1. Map of Lake Malawi/Nyasa, showing thermistor sites (THRM) and locations of meteorological station (M). The meteorological station shown at Monkey Bay was aboard the R/V/ *Usipa*, and collected data from around the lake during research cruises.

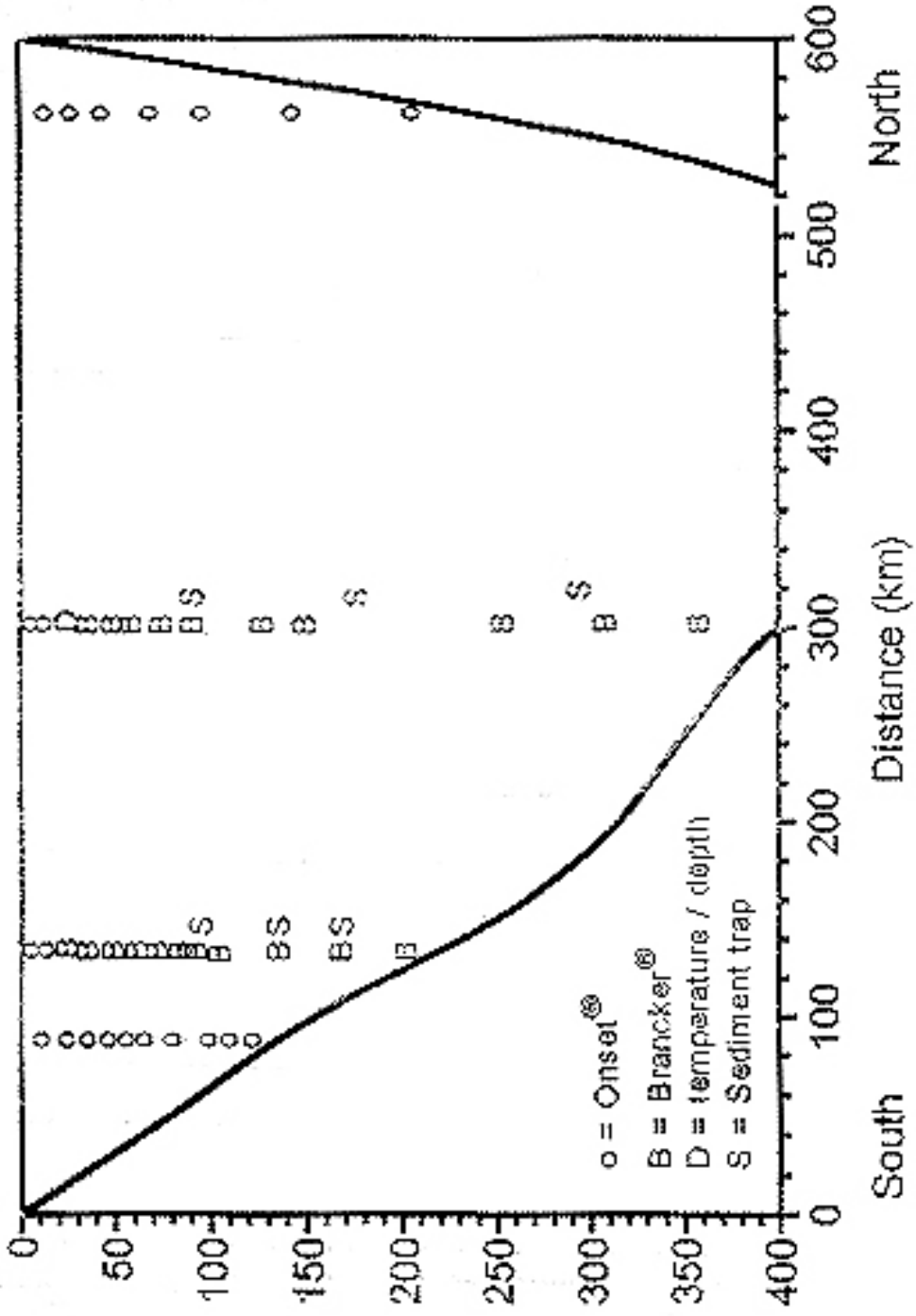

Fig. 5.2. Longitudinal section of lake showing positions of the thermistor loggers of various manufacturers. Brancker® loggers are accurate to within 0.08 °C, while Onset® loggers are accurate within 0.2 °C

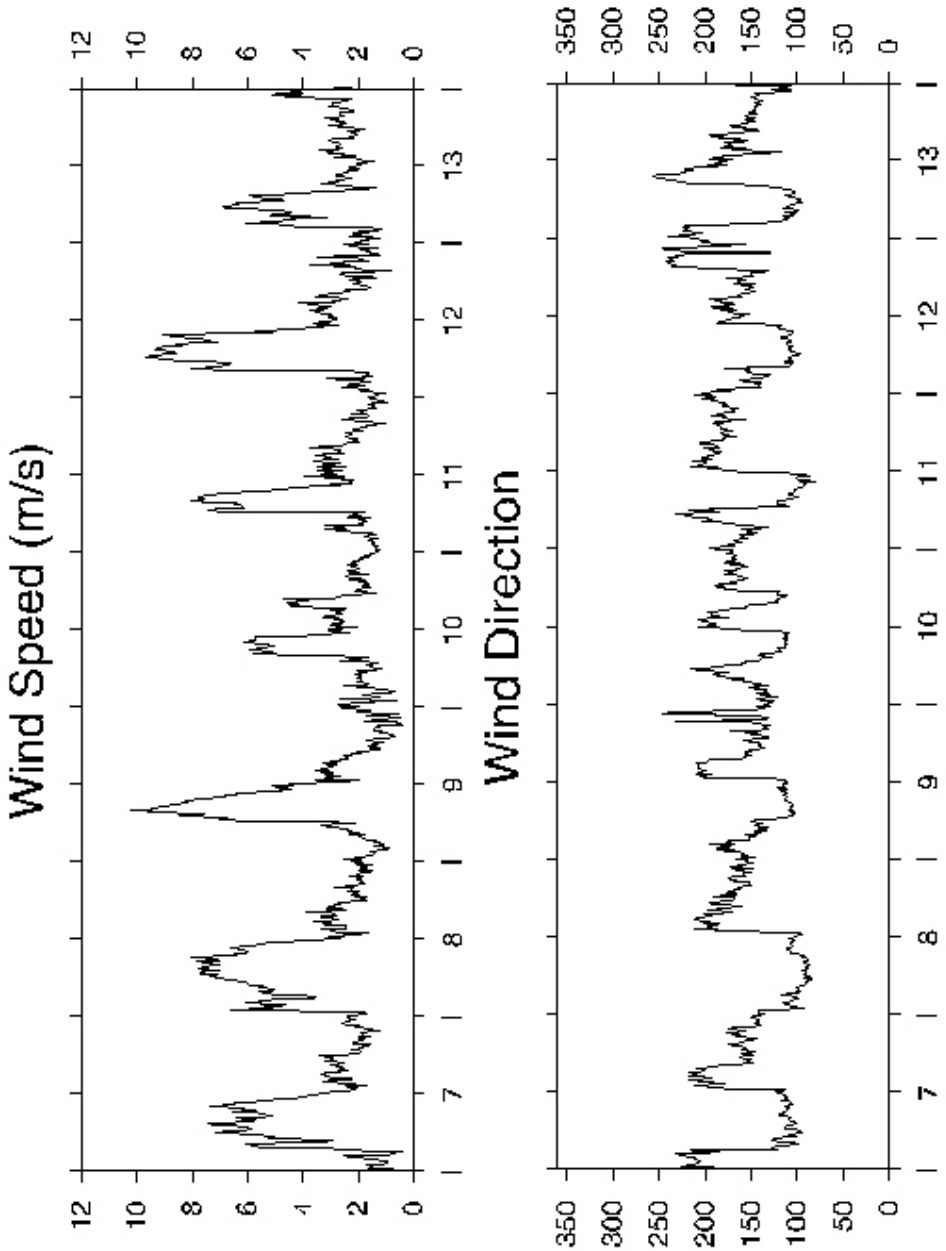

Fig. 5.3. Wind speed (top panel), wind direction (bottom panel) on a 10-minute basis at the Chilumba meteorological station from March 7 to 13, 1997.

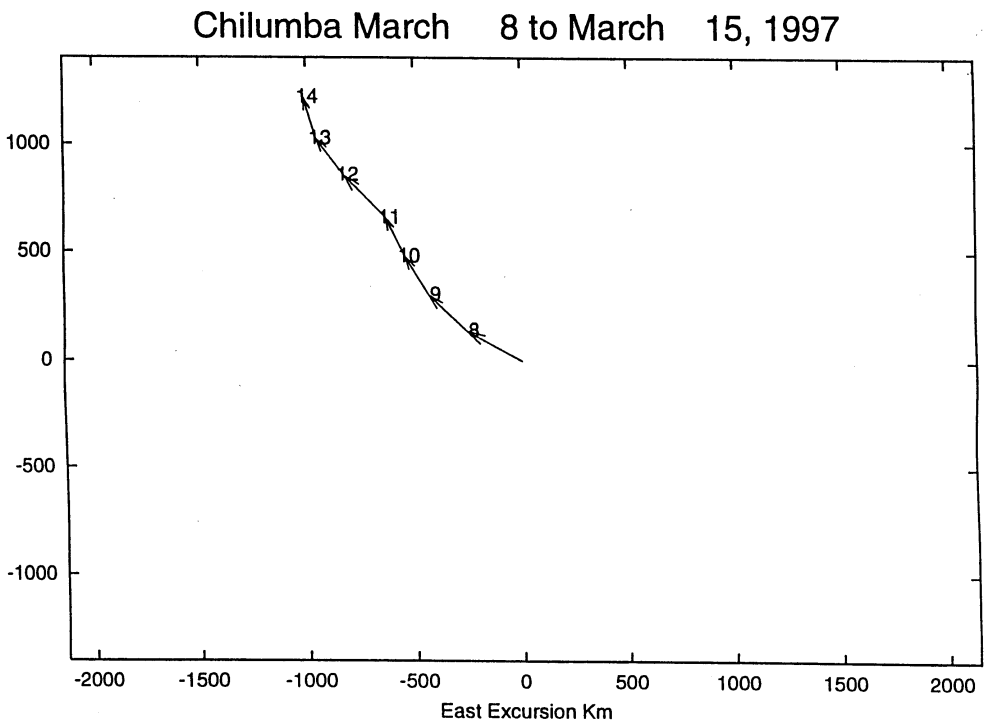

Fig. 5.4. Daily averaged wind trajectories for the Chilumba station, corresponding to the winds from March 8 to March 15, 1997, shown in Fig. 5.3.

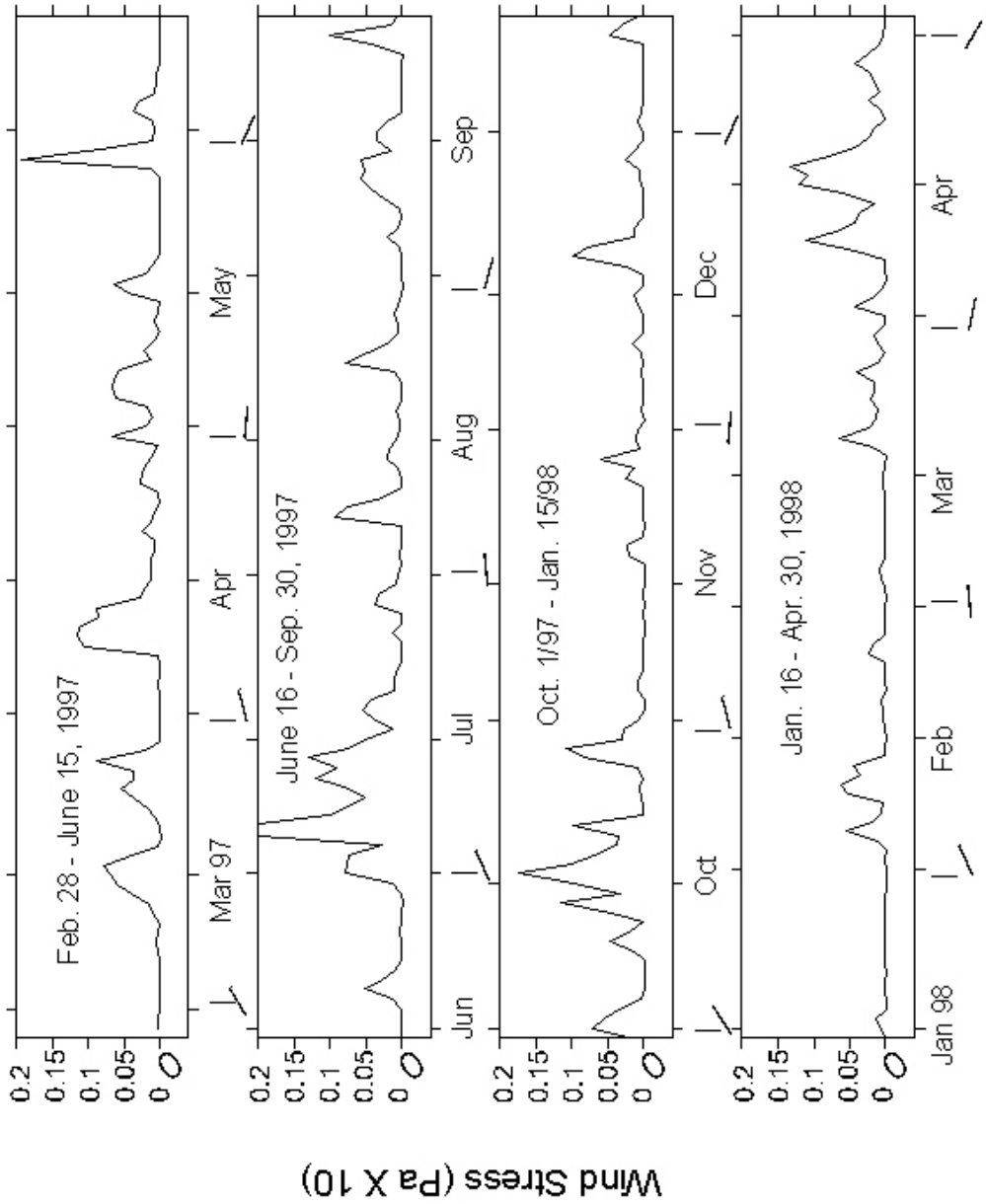

Fig. 5.5. Daily averaged wind stress at Senga Bay. Component along the major axis (positive to 0°) of the lake.

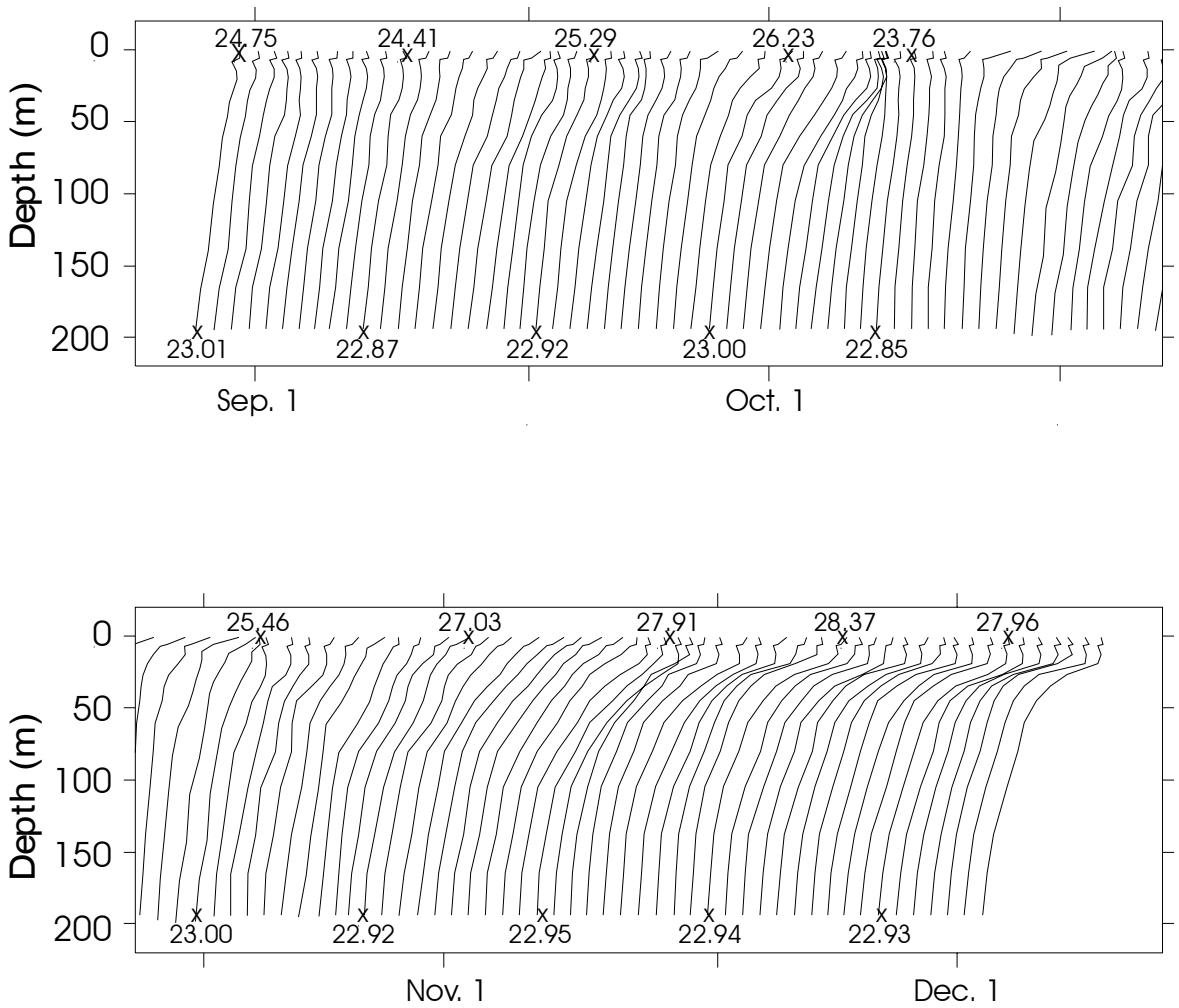

Fig. 5.6. Staggered profiles of daily averaged temperature at station THRM2, September 9 - October 14, 1997. The surface and bottom temperatures of every tenth profile are indicated on the profile.

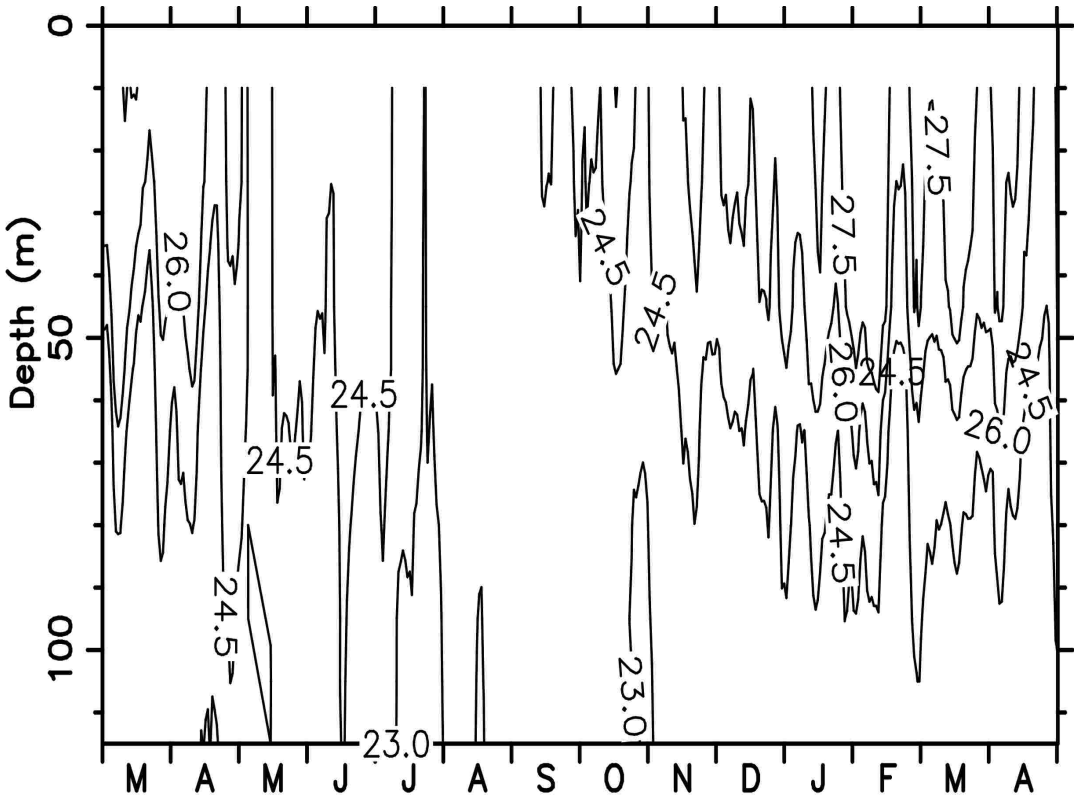

Fig. 5.7. Selected daily averaged isotherms as a function of depth and time at station THRM1, from March 1997 toApril 1998.

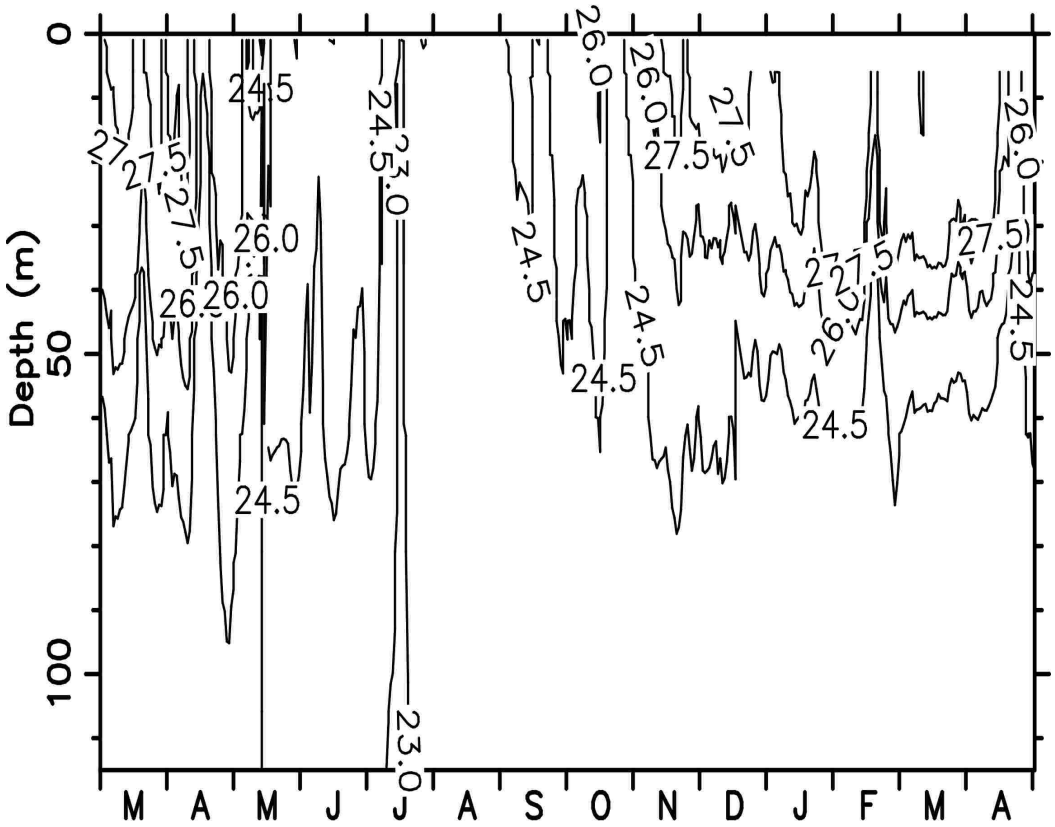

Fig. 5.8. Selected daily averaged isotherms as a function of depth and time at station THRM2, from March 1997 to April 1998.

The noted temperature difference between these stations suggests that water solutes and particles may be driven by a balance between surrface wind stress and these persistent temperature or density gradients. Direct comparisons of density differences were not possible as temperatures were not observed at the same depths at the two stations. Instead, temperatures were interpolated linearly at station THRM2 to the depths of stations THRM1 as indicated in Figure 5.2. Next, temperatures were used to calculate water density according to the standard lake water formula of Chen and Millero (1978) ignoring any contributions to density from total dissolved solids. This was justified on the basis of some test calculations which indicated that in the relatively shallow waters measured by the thermistor chains, salinity has a negligible effect on density. Salinity was determined from conductivity and temperature according to the relations of Wüest et al. (1996). Finally, profiles of the daily averaged buoyancy force, $\frac{g}{\overline{\rho}}\frac{\partial \rho}{\partial x}$, between moorings THRM1 and THRM2 were calculated by multiplying the horizontal density gradient, $\frac{\partial \rho}{\partial x}$, by the acceleration of gravity, g, and dividing by the average density, $\overline{\rho}$. This gradient was based on the 45 km separation between stations THRM1 and THRM2. A typical example is shown in Figure 5.9.

Analysis

Upwelling. The thermistor chain, the AVHRR surface temperature data and the daily averaged wind vectors were synthesized in four plots each showing a single satellite overflight, the nearest temperature profile data to the time of the temperature image and the preceding five days of winds. The wind trajectories in Figures 5.10 have been scaled by 6% in order to fit on the map of the lake. This factor corresponds to twice the usual rule-of-thumb for surface wind drift currents which typically have speeds about 3% of the wind speed. The days displayed were selected at random over the period from May through August, 1997, a period when our satellite receiving station was functioning well and the sky was relatively free of clouds. Winds at Likoma Island appear to be consistently underestimated, perhaps due to local sheltering. Unfortunately, one of the four meteorological stations and a thermistor mooring were inoperative during this period, but with the remaining good data it is still possible to draw some conclusions.

Remarkably, all four instances show that the coldest water is located in the southern extremity of the lake, that the isotherms are tilted downwards along the axis of the lake in a southerly direction, and that the wind field is southerly and nearly uniform along the length of the lake. This pattern of temperature and wind suggests that flows at the surface are directed to the north, that a weaker return flow occurs at depth in a southerly direction and that a downwelling flow in the northern half accompanied by an upwelling flow in the southern portion of the lake connect these two horizontal flows. If the strength of these flows could be determined as they respond to fluctuations in the wind speed and buoyancy gradients, then the advective flux of nutrients from deeper to shallower layers could be estimated.

Model Formulation. We lacked the resources to directly measure profiles of the horizontal flow at several location in the lake, which would be the minimum required to empirically infer from flow continuity considerations the vertical flows that would transport nutrients. Instead, we formulated a simple mathematical model of the wind and pressure driven flow in a vertical plane oriented along the longitudinal axis of the lake, similar to that of Findikakis and Street (1982), except that in our model internal pressure gradients were specified from the field observations via the buoyancy profiles instead of from the model. Because we input observed winds and buoyancy to the model and employed depth dependent eddy viscosities (vertical mixing coefficients), the equations of motion had to be solved numerically, unlike the purely analytical approach of Findikakis and Street (1982). Eddy viscosity was assumed to vary in the upper 10m according to the standard wall-law value based on the wind speed, and to be fixed at 10^{-5} m^2 s^{-1} below 10 m for all time.

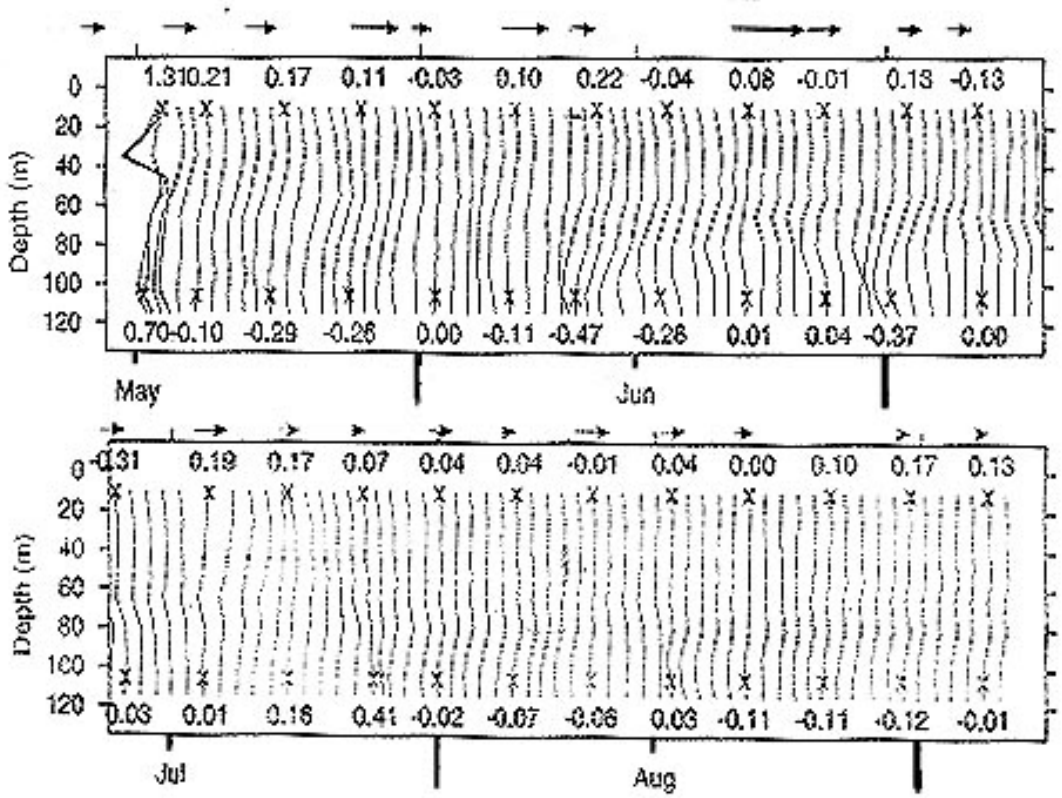

Fig. 5.9. Staggered daily buoyancy profiles between stations THRM1 and THRM2. Wind stress components are indicated by arrows at tops of plots. Notice that the two plots are contiguous in time. The surface and bottom values are indicated for every fifth profile.

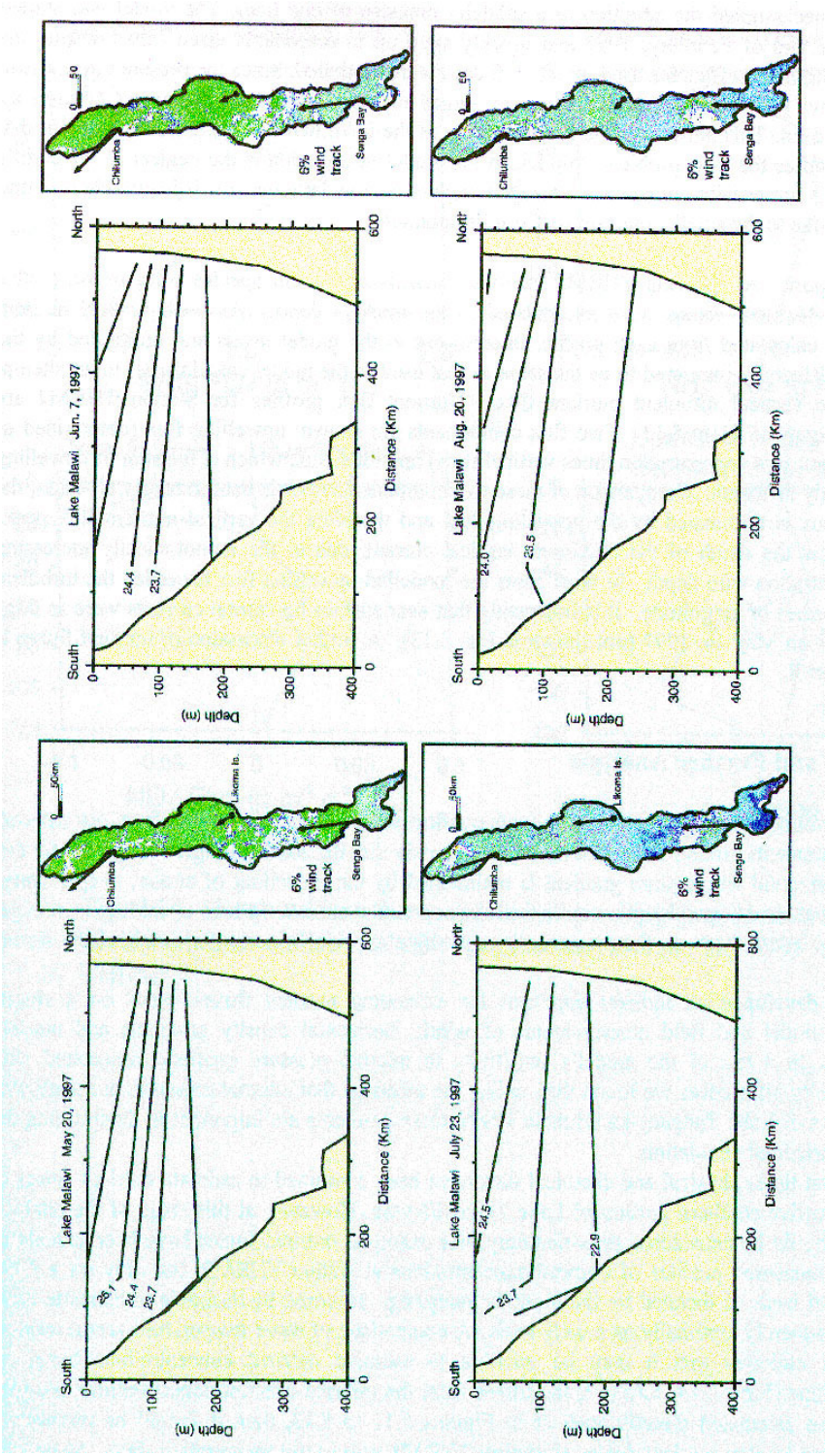

Fig. 5.10. AVHRR (NOAA satellite) thermal maps, longitudinal temperature section, and scaled (6%) wind excursions for four dates between May 20 and August 20, 1997. Wind excursions represent the five day period preceding the date indicated. The coloured areas represent various temperatures corresponding to the surface temperatures indicated in the accompanying longitudinal temperature cross sections (green is warmer, dark blue is cooler). White areas are cloud covered.

Near-surface eddy coefficients ranged from 10^{-2} to 10^{-4} m^2 s^{-1}. While daily averaged wind stress and buoyancy drove the model and the modelled flows were captured on a daily basis, numerical stability considerations necessitated the adoption of a subdaily timestep of one hour. The model was started from rest at the end of February, 1997 and quickly spun up to reasonably sized flows despite the relatively low mixing coefficients used. In all, 430 days were modelled. Since the present interest is in the internal flow field we ignored the transient surges of flow throughout the water column by imposing a rigid lid. This allows for the determination of the unknown surface pressure gradient that completely specifies the flow problem. Implicit in the model formulation is the neglect of the earth's rotation which is not possible in laterally averaged models. At low latitudes this is justifiable to a first approximation due to the small values of the Coriolis parameter.

Nutrient transport. At mooring THRM2 up to six dissolved nutrient species were profiled on a monthly basis. Nutrient values were interpolated to the model's depths. As well, vertical nutrient gradients were calculated from each profile, interpolated to the model levels and multiplied by the vertical eddy diffusivity (assumed to be the same as that used in the model calculations) in an attempt to estimate the vertical turbulent nutrient flux. Nutrient flux profiles for Station THRM2 are illustrated in Figures 5.11 to 5.13. Two flux components are shown; upwelling flux (determined as the product of nutrient concentration times vertical flow) and total flux, which is the sum of upwelling and vertical eddy diffusion. Comparison of these two components reveals that, in nearly all cases, the metalimnion flux is dominated by the upwelling flux and therefore the vertical nutrient flux peaks somewhat below the depth of the maximum vertical current, due to the monotonically increasing nutrient concentration with depth. In most cases the modelled upwelling flux exceeded the turbulent flux by three orders of magnitude. It is interesting that near surface horizontal currents were as large as 20 km day^{-1} on May 14, 1997 (not shown in Fig. 5.13). A further discussion of nutrient fluxes is given in Chapter 8.

Conclusions and Further Analysis

Nearly continuous water temperature records confirm what would be expected from our network of wind measurements around Lake Malawi/Nyasa, namely that the southern region is cooler and that the surface horizontal temperature gradient is maintained by the upwelling of cooler, deeper water. The temporal pattern of upwelling is unlike that of temperate zone lakes where upwelling is stronger but much more intermittent. In the present case upwelling appears to occur for much of the annual cycle.

We have developed an indirect approach for estimating nutrient fluxes based on a simple mathematical model and field measurements of winds, horizontal density gradients and nutrient concentrations. In a test of the model's sensitivity to internal pressure gradients associated with horizontal density differences we found that, unlike the assertion that internal pressures are negligible in the dynamics of Lake Tanganyika (Huttala 1997), these gradients are important in determining the vertical and horizontal circulation.

For the first time, physical and chemical data have been combined to estimate nutrient fluxes in the most productive southern portion of Lake Malawi/Nyasa. However, at this stage of the analysis our findings should be considered as preliminary. For example, nutrient fluxes have been calculated from directly measured profiles of nutrient concentrations at station THRM2, but only on a fairly coarse temporal basis as dictated by the monthly sampling. It would be desirable to estimate these fluxes more frequently, optimally on a daily basis. A comparison of water temperature versus nutrient concentrations indicates that it may be possible to estimate nutrient concentrations based on temperature alone (Figs. 5.14, 5.15). If the fluxes from the inferred nutrient concentrations compare well with those calculated directly such as in Figures 5.11 to 5.13, then it should be possible to estimate the day-by-day nutrient fluxes at station THRM2 using only temperature data. Moreover, this approach suggests that similar nutrient fluxes could be estimated at the other thermistor stations, providing reasonable correlations between temperature and nutrient concentrations are found.

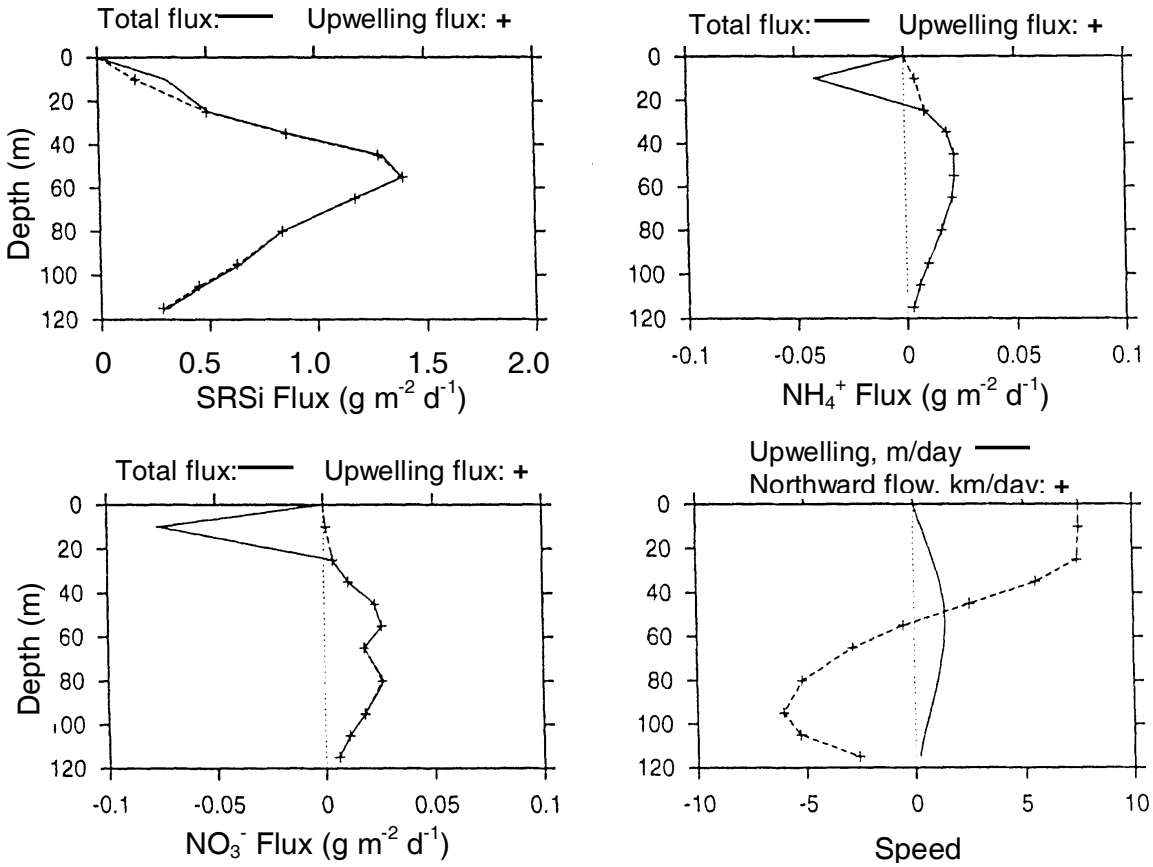

Fig. 5.11. Total nutrient flux (solid line), upwelling flux (dashed line), and horizontal and vertical velocity profiles for March 21, 1997 at station THRM1.

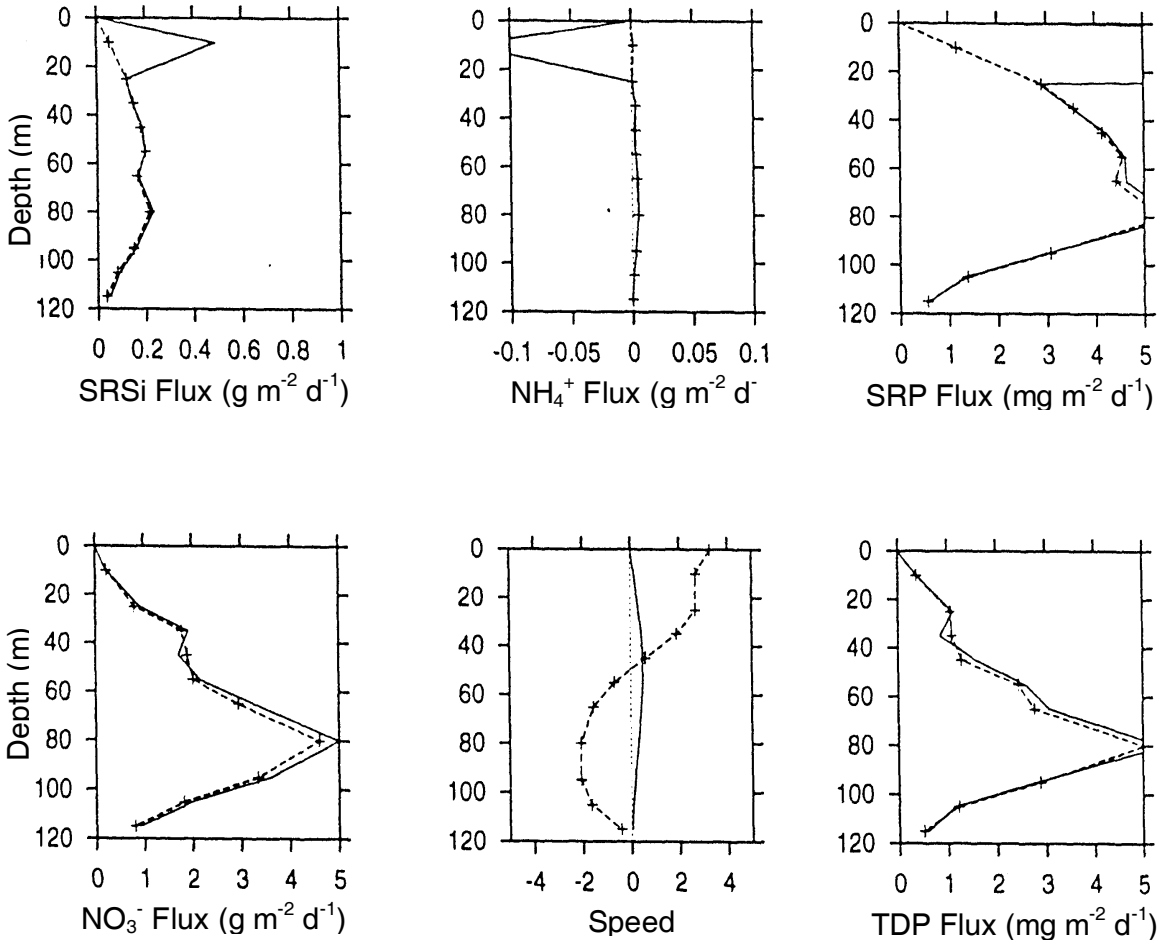

Fig. 5.12. Total nutrient flux (solid line), upwelling flux (dashed line), and horizontal and vertical velocity profiles for April 29, 1997 at station THRM1.

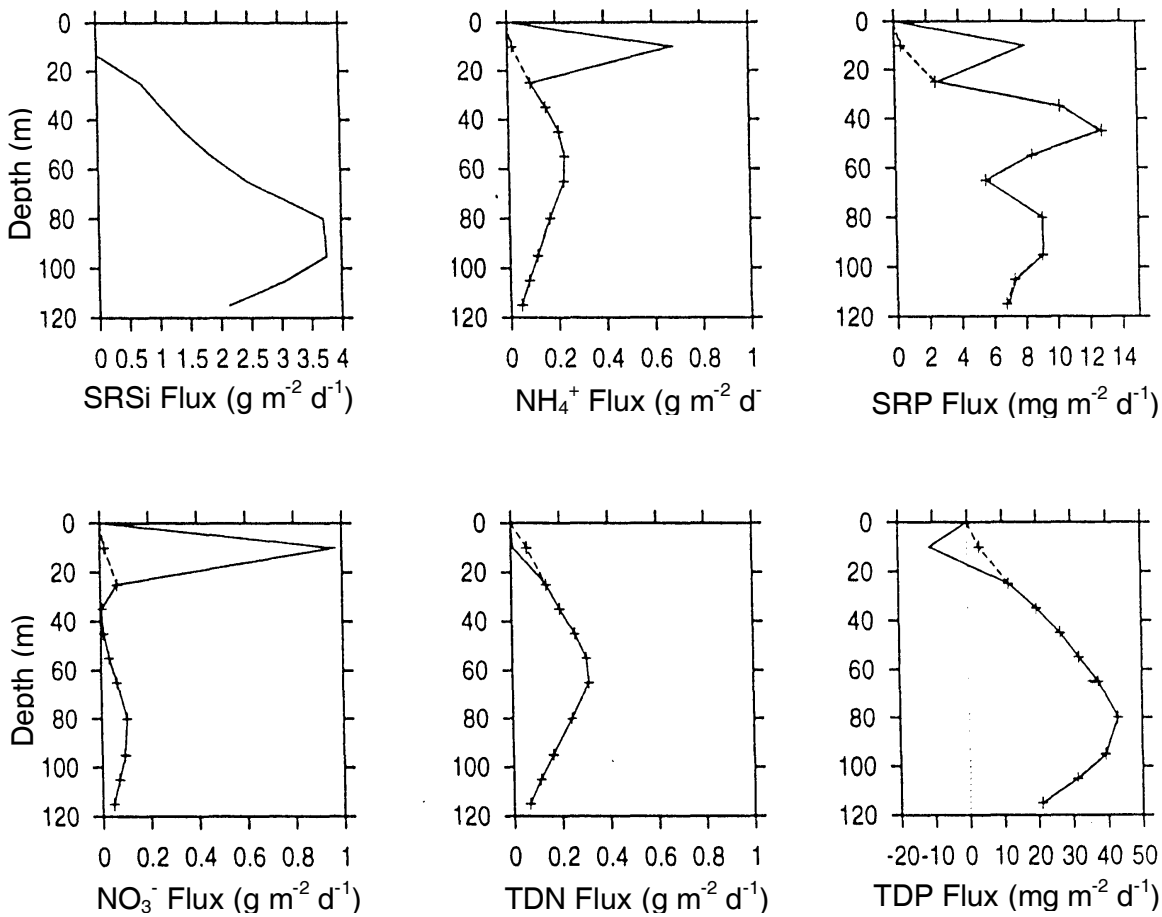

Fig. 5.13. Total nutrient flux (solid line) and upwelling flux (dashed line) for May 14, 1997 at station THRM1.

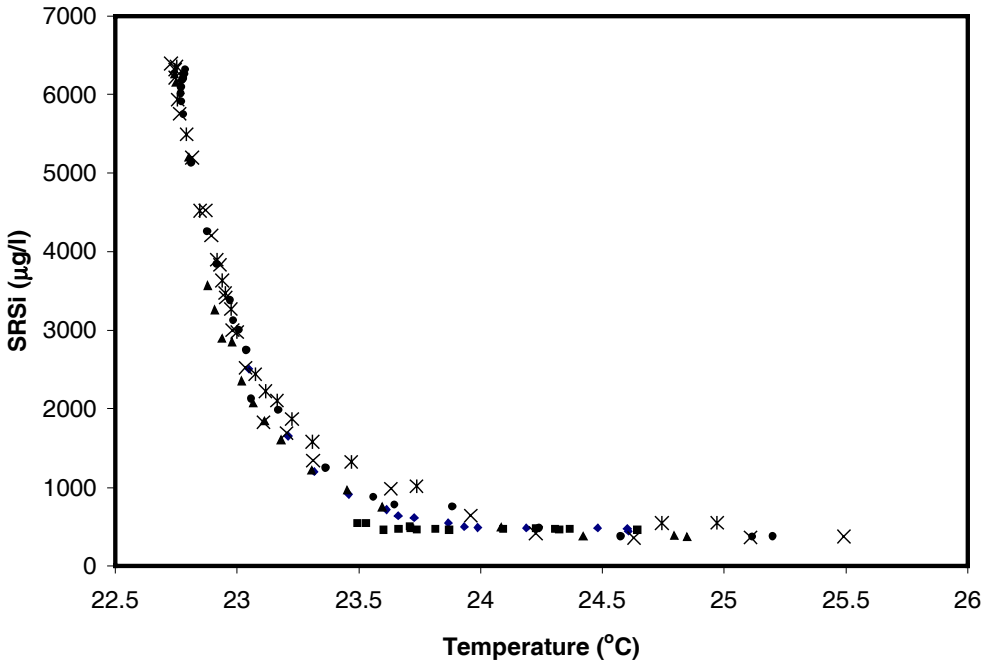

Fig. 5.14. Scatter plot of soluble reactive silica concentration vs. water temperature, using data from five deep profiles at various stations in September 1997.

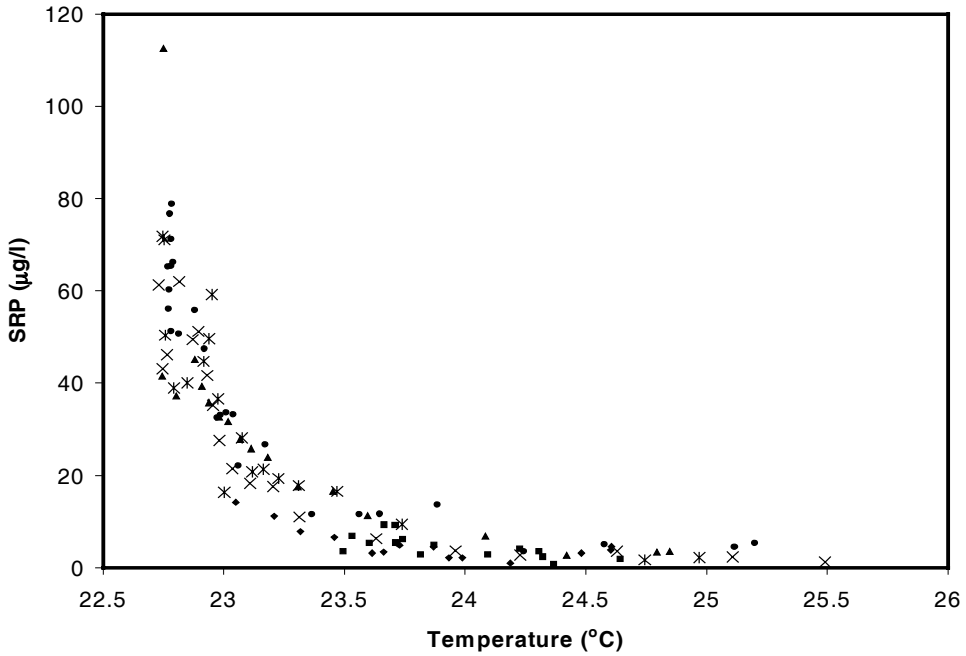

Fig. 5.15. Scatter plot of soluble reactive phosphorus concentration vs. water temperature, using data from the same times and locations as for Fig. 5.14.

We hope to further investigate the validity of some of the assumptions used in the analysis. For example, it would be useful to know if the extrapolation of land-based winds to the open lake is reasonable. An independent check on the magnitude of the assumed vertical mixing coefficients by means of the data discussed in Chapter 4 would be extremely valuable.

In the longer term we hope to develop three-dimensional circulation and chemical transport models for Lake Malawi/Nyasa which would assist ongoing monitoring studies on the lake and be useful predictive tools.

References

Beauchamp, R.S.A. 1953. Hydrological data from Lake Nyasa. J. Ecol. 41: 226-239.

Bootsma, H. 1993. Algal dynamics in an African Great Lake, and their relation to hydrographic and meteorological conditions. Ph.D. Thesis, Universtiy of Manitoba, 311 pp.

Chen, C.T, and Millero, F.J. 1977. The use and misuse of pure water PVT properties for lake water. Nature, 266: 707–708.

Eccles, D.H. 1974. An outline of the physical limnology of Lake Malawi (Lake Nyasa). Limnology and Oceanography 19: 730-742.

Findikakis, A.N., and R.L. Street. 1982. Vertical structure of internal modes in stratified flows ASCE Journal of Hydrological Engineering 108: 583-595.

Huttula, T. 1997. Flow, thermal regime and sediment transport studies in Lake Tanganyika. Kuopio University Pub. C. Natural and Environmental Sciences 73.

Jackson, P.B.N., T.D. Iles, D. Harding and G. Fryor. 1963. Report on the survey of northern Lake Nyasa, 1954-1955. Malawi Government Printer, Zomba.

Patterson, G, and O. Kachinjika. 1995. Limnology and phytoplankton ecology. Pages 1-67 In Menz, A. (ed.), The fishery potential and productivity of the pelagic zone of Lake Malawi/Niassa. Chatham, UK: Natural Resources Institute.

Wüest, A.,G. Piepke and J.D.Halfman, 1996 Combined effects of dissolved solids and temperature on the density stratification of Lake Malawi. Pages 183-202 *In* Johnson, T.C., and E.O. Odada (eds.), The limnology, climatology and paleoclimatology of the East African lakes. Gordon and Breach, Amsterdam.